J Paleolimnol (2023) 69:213–230
https://doi.org/10.1007/s10933-022-00269-2

ORIGINAL PAPER

# Abrupt diatom responses to recent climate and land use changes in the Cantabrian Mountains (NW Spain)

**Jon Gardoki · Mario Morellón · Manel Leira · Francisco Javier Ezquerra · Juan Remondo · Willy Tinner · María Luisa Canales · Anouk van der Horst · César Morales-Molino**

Received: 2 July 2021 / Accepted: 25 August 2022 / Published online: 3 October 2022


**Abstract** The multi-proxy study of sediment cores from Lake Isoba (43° 02′ N, 5° 18′ W; 1400 m a.s.l.) allows a detailed assessment of the past hydrological and environmental dynamics in north-western Iberia resulting from the interplay between climate variability and anthropogenic impact. The combination of diatom stratigraphy, sedimentology and high-resolution elemental geochemistry along with a robust chronological framework (established by $^{210}$Pb, $^{137}$Cs and $^{14}$C dating) provides a detailed environmental reconstruction for the past ~ 500 years. Abrupt changes in the fossil diatom assemblages indicate a high sensitivity of this small lake to past environmental change and allow identifying four major stages related to the main climate fluctuations of the Little Ice Age (LIA)

J. Gardoki (✉)
Departamento de Geología, Facultad de Ciencia y Tecnología, Universidad del País Vasco UPV/EHU, Barrio Sarriena S/N, 48940 Leioa, Biscay, Spain
e-mail: jon.gardoqui@ehu.eus

J. Gardoki · M. Morellón · M. L. Canales
Departamento de Geodinámica, Estratigrafía y Paleontología, Facultad de Ciencias Geológicas, Universidad Complutense de Madrid, C/ José Antonio Novais 12, 28040 Madrid, Spain
e-mail: mmorello@ucm.es

M. L. Canales
e-mail: mcanales@ucm.es

M. Leira
BioCost Research Group, Facultade de Ciencias and Centro de Investigacións Científicas Avanzadas (CICA), Universidade da Coruña, 15071A Coruña, Spain
e-mail: m.leira@udc.es

M. Leira
Biodiversity and Applied Botany Research Group, Departamento de Botánica, Facultade de Bioloxía, Universidade de Santiago de Compostela, 15782 Santiago de Compostela, Spain

F. J. Ezquerra
Consejería de Medio Ambiente, Vivienda y Ordenación del Territorio, Junta de Castilla y León, C/ Rigoberto Cortejoso 14, 47014 Valladolid, Spain
e-mail: ezqbotfr@hotmail.es

J. Remondo
DCITIMAC, Facultad de Ciencias, Universidad de Cantabria, Avda. de los Castros s/n, 39005 Santander, Spain
e-mail: juan.remondo@unican.es

W. Tinner · A. van der Horst · C. Morales-Molino
Institute of Plant Sciences & Oeschger Centre for Climate Change Research, University of Bern, Altenbergrain 21, 3013 Bern, Switzerland
e-mail: willy.tinner@ips.unibe.ch

A. van der Horst
e-mail: anouk.vanderhorst@students.unibe.ch

C. Morales-Molino
e-mail: cesar.morales@uah.es

C. Morales-Molino
Grupo de Ecología y Restauración Forestal, Departamento de Ciencias de La Vida, Facultad de Ciencias, Universidad de Alcalá, Campus Universitario, 28805 Alcalá de Henares, Spain

and recent warming. High lake levels, enhanced runoff and higher productivity characterised the middle phase of the LIA (~ 1550 to 1630 CE), indicating an overall wet climate. Conversely, shallow lake levels, decreased runoff and relatively low productivity prevailed during the last phase of the LIA and the onset of the Industrial Era (~ 1630 to 1925 CE), likely due to colder and drier conditions. High lake levels and higher carbonate input occurred after ~ 1925 CE until the 1980s CE, when our data show an abrupt drop in lake levels probably caused by a regional negative rainfall anomaly related to climate warming during the past decades. Finally, since ~ 1997 CE a remarkable and abrupt increase in the lake nutrient load and turbidity is detected, probably associated with the replacement of transhumant sheep flocks with staying cattle. The main environmental changes reconstructed at Lake Isoba mostly agree with other palaeoclimatic records from northern Spain. However, the hydrological patterns reconstructed are opposed to those observed on the northern slopes of the Cantabrian Mountains. The recent and strong impact of land-use changes on the lake, causing more ecological disruptions than previous climate changes, is noteworthy and demonstrates the high sensitivity of mountain lakes to human activities in a global change context.

**Keywords** Lake sediments · Late Holocene · Climate change · Transhumance · Eutrophication

## Introduction

Mountain lakes are highly sensitive and vulnerable to environmental changes. Disturbances slightly exceeding the natural range of variability can cause dramatic hydrological shifts, which in turn may lead to complex changes in the composition of their biological communities (Cohen 2003; Kuefner et al. 2020). Diatoms are the most abundant algae in lakes and feature highly specific ecological requirements even at species level, particularly concerning hydrochemistry and habitat (Stoermer and Smol 1999). Thus, changes in the hydrological conditions of mountain lakes occurring on annual to decadal timescales have critical effects on their diatom communities. In summary, diatoms' ubiquity and good preservation in lacustrine environments, their high speciation rate and rapid response make them excellent sentinels of both natural and human-driven environmental changes (Stoermer and Smol 1999; Cohen 2003).

The Cantabrian Mountains (NW Spain; Fig. 1a, b) constitute an ideally suited area for the study of recent environmental fluctuations. Their location on the boundary between the Atlantic and Mediterranean biogeographic realms, and therefore in a climatically transitional area between humid (north) and dry (south) summers, makes them highly sensitive to climate change. Additionally, this area has a long history of human occupation and changing land use. During the last centuries, transhumant shepherding and cattle ranching played a prominent role in the regional economy, with mining activities and tourism increasing their importance more recently (Ezquerra et al. 2005). Despite the number of palaeolimnological reconstructions using diatoms has increased significantly over the last decades in the Iberian Peninsula (Catalán et al. 2002; Vegas-Villarrúbia et al. 2013; Jambrina-Enríquez et al. 2014), very few studies have been carried out in the Cantabrian Mountains (López-Merino et al. 2011; Moreno et al. 2011). Consequently, considerable gaps in our knowledge about the main drivers of recent environmental change in this area and their impact in lake systems persist.

In this paper, we investigate the responses of diatom communities to recent climatic variability and anthropogenic disturbance based on the multi-proxy analysis (diatom stratigraphy, sedimentology and geochemistry) of sediment cores from Lake Isoba (*'Lago de Isoba'* in Spanish; named 'Isoba' onwards), a mountain lake located on the southern slopes of the Cantabrian Mountains (NW Spain; Fig. 1b). A robust chronology based on numerous radiometric dates ($^{137}$Cs, $^{210}$Pb and $^{14}$C) allows a detailed and precise reconstruction of the environmental history of the region for the past ~ 500 years. Furthermore, this multi-proxy approach has allowed us to unravel recent hydrological changes in the region and assess their natural or anthropic forcing.

## Study area

Isoba (43° 02′ N, 5° 18′ W; 1400 m a.s.l.) is a small permanent shallow lake (2.86 ha, 6 m maximum water depth) of glacio-karstic origin, located on the southern slopes of the western sector of the Cantabrian Mountains (NW Iberian Peninsula) (Fig. 1a, b).

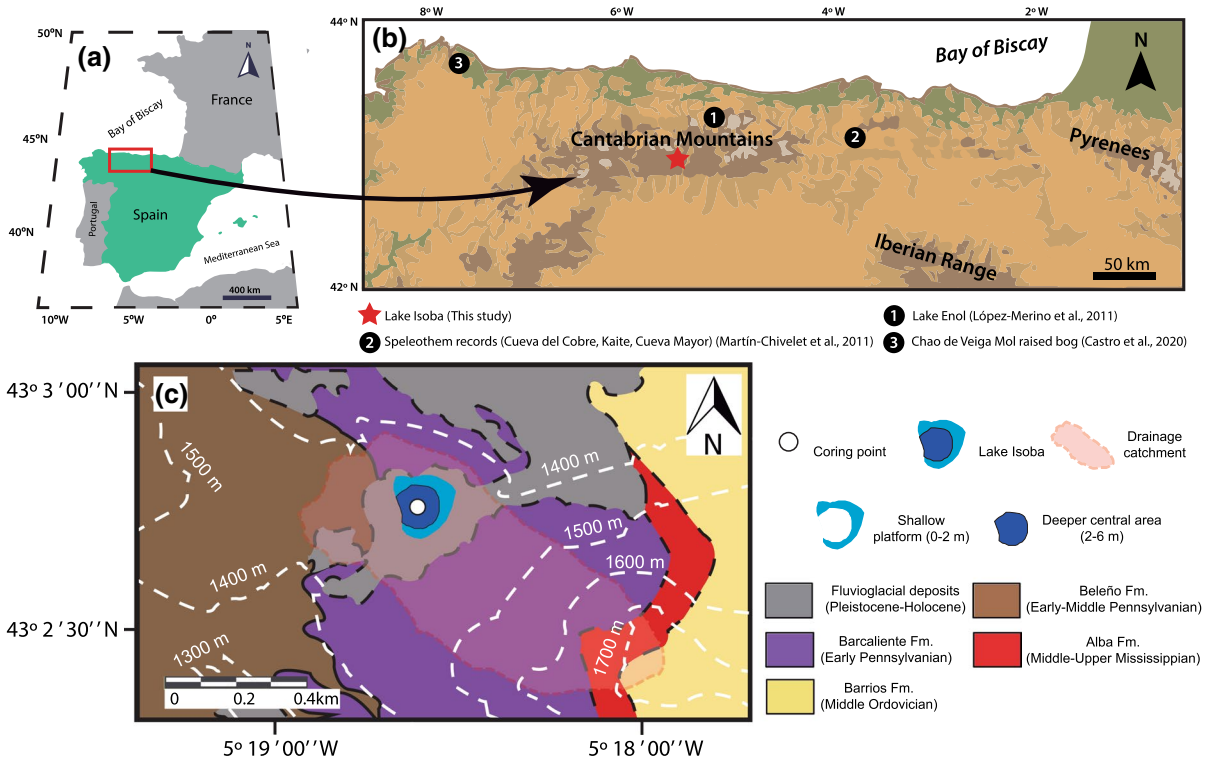


**Fig. 1** **a** Location of the Cantabrian Mountains in the Iberian Peninsula. **b** Location of Lake Isoba and other significant palaeoclimatic records mentioned in the text. **c** Geological map of the Lake Isoba catchment and surroundings

The catchment lies on an intensely deformed Palaeozoic stratigraphic series of the northernmost part of the Iberian Massif, in the Cantabrian Zone (Álvarez-Marrón et al. 1988). In the drainage basin, bedrock mostly consists of black laminated limemudstones from the Barcaliente Formation (Early Pennsylvanian), overlaid by Pleistocene-Holocene fluvio-glacial deposits (Álvarez-Marrón et al. 1988). Isoba is a closed basin without any surface outlet and just minor temporary inlets streams. Sediment input is derived from the bedrock weathering and soil erosion within the catchment, latter transported into the lake by surface run-off and snow melt.

Isoba shows a nearly circular basin (~ 170 m diameter; Fig. 1c), which can be divided into two different zones: an extensive shallow peripheral platform (0–2 m water depth) and a deeper central area (2–6 m water depth). In the shallow platform two rings of macrophytic vegetation occur: the outer mainly consists of helophytes such as *Carex rostrata* Stokes, *Glyceria fluitans* (L.) Brown and *Eleocharis uniglumis* (Link) Schult., while the inner is dominated by *Potamogeton natans* L., mixed with *Myriophyllum alterniflorum* D.C., *Groenlandia densa* (L.) Fourr. and *Chara vulgaris* L. (Fernández-Aláez et al. 1987). Aquatic vegetation is not so dense in the deeper central part of the lake. Lake water has a relatively low electrical conductivity (196 µS $cm^{-1}$) and pH is about 8.5.

The regional climate is Mediterranean-temperate cool and wet (Ortega Villazán and Morales Rodríguez 2015). Mean annual precipitation at the Puerto de San Isidro pass (1520 m a.s.l.), ~ 5.7 km away from Isoba, is 1516 mm, while mean annual temperature is 5.8 °C. Seasonal changes in temperature are moderate, with winter (January) and summer (July and August) average temperatures of 0.1 °C, and 12.7 °C, respectively (Ortega Villazán and Morales Rodríguez 2015). For several centuries, the area was subject to an intense use as summer pastures by massive transhumant flocks of merino sheep. This traditional land use has left a strong imprint in the current

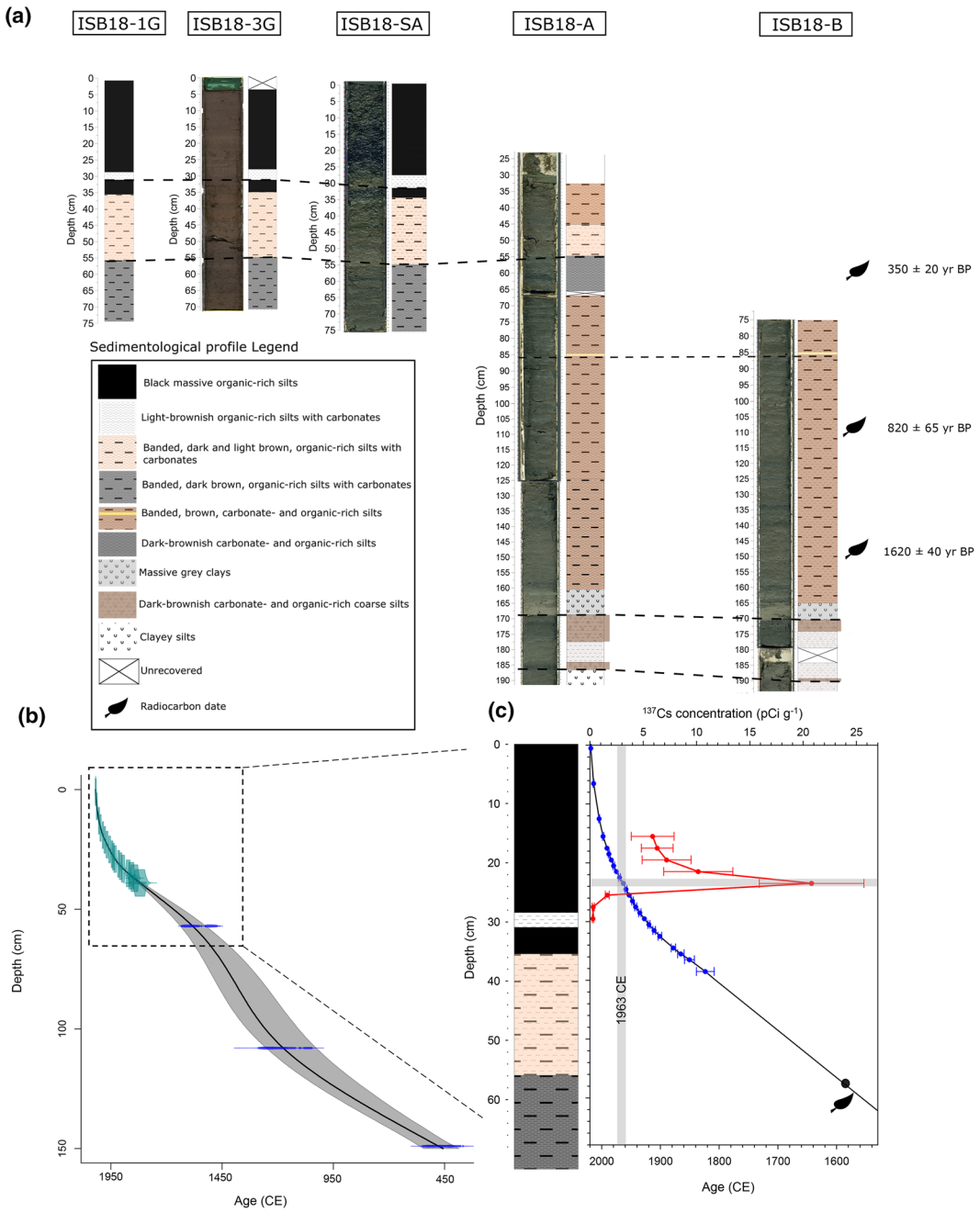


**Fig. 2** **a** Lithostratigraphic correlation of the Lake Isoba cores ISB18-1G, ISB18-3G, ISB18-SA, ISB18-A and ISB18-B. The depth scale corresponds to the depth of the master core. **b** Age-depth model of the upper section of the Isoba sequence based on smoothing spline of $^{210}$Pb and $^{14}$C dates. **c** Detailed age-depth relationship of the studied section, showing the location of the $^{210}$Pb dates and the $^{137}$Cs concentration profile. The line represents the interpolated interval between the $^{210}$Pb and the $^{14}$C dates

high-elevation vegetation of the Cantabrian Mountains, largely consisting in grasslands, meadows and shrublands.

## Materials and methods

### Sampling and sedimentological analysis

In 2018, we retrieved three sediment cores (ISB18-SA; 76 cm long, ISB18-A-1G; 75 cm long, ISB18-A-3G; 71 cm long) from the deepest area of Lake Isoba (43° 02′ 44.8″ N, 5°, 18′ 52.9″ W), using a UWITEC gravity corer operated from a floating platform. Two additional long cores (ISB18-A and ISB18-B) were also recovered using a modified Livingstone piston corer. Cores ISB18-SA, ISB18-A and ISB18-B were split lengthwise, photographed, and correlated according to their lithostratigraphy to produce a composite master core (Fig. 2a). In the field, we subsampled in situ the core ISB18-A-1G into 1cm thick slices for $^{210}$Pb and $^{137}$Cs dating. During subsampling, we annotated the location of any distinct lithostratigraphic layer in ISB18-A-1G enabling its latter correlation with the composite master core. Diatom analyses were carried out in the uppermost 60 cm of core ISB18-SA, whereas geochemical and compositional analyses were performed on core ISB18-A-3G. Sedimentary facies were defined by visual macroscopic description and microscopic observation of smear slides following Schnurrenberger et al. (2003).

The chronology of the sequence is based on $^{137}$Cs and $^{210}$Pb dating of the core ISB18-A-1G by gamma ray spectrometry, along with three Accelerator Mass Spectrometry (AMS) $^{14}$C dates on terrestrial plant macrofossils from the master core ISB18. Lead-210 dates were determined using the Constant Rate of Supply model (Appleby 2001). The radiocarbon dates were converted into calendar years using the INTCAL20 calibration curve (Reimer et al. 2020). An age-depth model for the studied section of the ISB18 sequence was constructed using a smoothing spline (95% confidence interval, 10,000 iterations, and smooth = 0.4) between the $^{210}$Pb and $^{14}$C dates using the package 'clam' version 4.0.3 (Blaauw et al. 2020) running in R environment.

### Diatom analysis

A total of sixteen sediment samples were extracted from ISB18-A core at 2–6-cm intervals and subsequently treated using 30% $H_2O_2$ and 10% HCl following Renberg (1990). The resultant suspension was mounted in Naphrax (®, refractive index = 1.74). At least 300 diatom valves per sample were counted on random transects (Battarbee et al. 2001). Valve concentrations per gram of dry sediment were calculated after adding a known amount of divinylbenzene microspheres (Battarbee 1986). Diatom valves identification mainly followed Krammer and Lange-Bertalot (1986, 1991), Lange-Bertalot (2000, 2005) and latter taxonomic updates in AlgaeBase (Guiry and Guiry 2020). The interpretation of the fossil diatom assemblages was based on the modern environmental requirements of the main taxa as detailed in Van Dam et al. (1994), Reynolds (2006) and Niyatbekov and Barinova (2018). Diatom results were expressed as percentages of the total number of valves counted in each sample. Planktonic/benthic (P/B) ratios also calculated. We delimited different Diatom Zones ('DZ') according to changes in the species and abundances shown in the assemblages. We also conducted a Correspondence Analysis (CA) on the diatom raw percentage data to assess relationships between species and samples using the package 'FactoMineR' version 2.4 in R. A Detrended Correspondence Analysis (DCA) was performed using the software PAST in order to validate CA consistency.

### Geochemical and compositional analyses

Core ISB18-A-3G was measured at 2-mm resolution for major, light elements using an AVAATECH X-Ray Fluorescence (XRF) core scanner (Universitat de Barcelona) with a 30-s count time at 10 kV (Si, Al, K, Ti, Ca, Mn and Fe) and 30 kV (Rb, Zr and Sr) X-ray voltage. The Si/Ti, Ca/Ti and (Zr + Rb)/Sr ratio were also calculated. Results for each element were expressed as counts per second. A Pearson correlation coefficient matrix between the elements was constructed using R. Additionally, samples were taken every 2 cm, freeze-dried and mechanically homogenised using an agate

mortar to measure total organic carbon (TOC) and total nitrogen (TN). These analyses were carried using a LECO CNS 928 analyser with previous acid digestion. Principal Component Analysis (PCA) and diagrams of geochemical-compositional raw data were carried out with the package 'FactoMineR' version 2.4 in R and Sigmaplot 11.0, respectively.

**Table 1** $^{210}$Pb and $^{14}$C dates of the Lake Isoba (Cantabrian Range, Spain) sedimentary record

| Sample depth (cm) | Laboratory code | Material | Total $^{210}$Pb activity (pCi g$^{-1}$) | Unsup. $^{210}$Pb activity (pCi g$^{-1}$) | Age (CE)[a] | Radiocarbon age (yr BP) | Calibrated age (CE), 95% CI[b] | Calibrated (CE), median |
|---|---|---|---|---|---|---|---|---|
| 0–1 | ISB 0–1 | Dry sediment | 20.963 ± 0.428 | 19.764 ± 0.429 | 2018 ± 0.65 | | | |
| 6–7 | ISB 6–7 | | 23.829 ± 0.393 | 22.630 ± 0.394 | 2014 ± 0.65 | | | |
| 12–13 | ISB 12–13 | | 24.255 ± 0.407 | 23.056 ± 0.409 | 2004 ± 0.76 | | | |
| 15–16 | ISB 15–16 | | 22.512 ± 0.511 | 21.313 ± 0.512 | 1997 ± 0.85 | | | |
| 18–19 | ISB 18–19 | | 22.595 ± 0.388 | 21.396 ± 0.389 | 1988 ± 1.08 | | | |
| 20–21 | ISB 20–21 | | 21.452 ± 0.419 | 20.253 ± 0.421 | 1979 ± 1.34 | | | |
| 22–23 | ISB 22–23 | | 16.595 ± 0.382 | 15.396 ± 0.383 | 1969 ± 1.57 | | | |
| 24–25 | ISB 24–25 | | 11.43 ± 0.396 | 10.231 ± 0.398 | 1958 ± 1.55 | | | |
| 26–27 | ISB 26–27 | | 7.711 ± 0.18 | 6.512 ± 0.183 | 1947 ± 1.44 | | | |
| 27–28 | ISB 27–28 | | 7.202 ± 0.159 | 6.003 ± 0.163 | 1941 ± 1.69 | | | |
| 28–29 | ISB 28–29 | | 7.398 ± 0.165 | 6.199 ± 0.168 | 1935 ± 2.07 | | | |
| 30–31 | ISB 30–31 | | 5.056 ± 0.205 | 3.857 ± 0.208 | 1919 ± 1.8 | | | |
| 31–32 | ISB 31–32 | | 4.186 ± 0.116 | 2.987 ± 0.121 | 1910 ± 2.32 | | | |
| 32–33 | ISB 32–33 | | 3.804 ± 0.097 | 2.605 ± 0.103 | 1900 ± 3.14 | | | |
| 34–35 | ISB 34–35 | | 2.734 ± 0.092 | 1.535 ± 0.098 | 1878 ± 3.66 | | | |
| 35–36 | ISB 35–36 | | 2.295 ± 0.07 | 1.097 ± 0.078 | 1865 ± 5.54 | | | |
| 36–37 | ISB 36–37 | | 1.764 ± 0.041 | 0.565 ± 0.053 | 1851 ± 8.41 | | | |
| 38–39 | ISB 38–39 | | 1.456 ± 0.031 | 0.257 ± 0.046 | 1825 ± 15.22 | | | |
| 56–58 | BE-18222 | *Cytisus oromediterraneus* twigs | | | | 350 ± 20 | 1524–1638 | 1583 |
| 105–111 | BE-17841 | *Betula* seed, bud scales indet., bark, deciduous leaf fragments | | | | 820 ± 65 | 1027–1252 | 1175 |
| 148–151 | BE-17842 | *Pinus* bud scale, conifer periderm, twig | | | | 1620 ± 40 | 406–562 | 477 |

*CI* Confidence interval

[a]The ages reported correspond to the mid-depth of the analysed interval

[b]IntCal20 (Reimer et al 2020), 'clam' (Blaauw et al 2020)

## Results

### Chronology

Total and unsupported $^{210}$Pb activity values are quite constant in the uppermost ~ 20 cm and then experience an abrupt decrease further down (Table 1). Unsupported $^{210}$Pb activity shows an overall decrease from the surface sample to 38.5 cm depth (from 19.764 ± 0.429 to 0.257 ± 0.046 pCi g$^{-1}$; Table 1). Thus, the chronology of the $^{210}$Pb-dated section (topmost 39 cm), is well constrained and suggests an age of 1825 CE at 38.5 cm depth (Fig. 2, Table 1). The $^{137}$Cs profile corroborates the $^{210}$Pb chronology, since the $^{137}$Cs peak corresponding to 1963 CE (23–24.5-cm depth) is bracketed by $^{210}$Pb dates (1959 CE at 24.5 cm and 1967 CE at 23 cm; Fig. 2b, c). The age-depth model including the $^{210}$Pb and the $^{14}$C dates (Table 1) dates the base of the studied section of the Isoba sedimentary sequence (65.5-cm depth) at ~ 1500 CE (Fig. 2a). The sedimentation rate shows an upcore increasing trend, ranging from 0.071 to 0.125 cm y$^{-1}$ in the lower part (65.5–30 cm), increasing to 0.25 cm y$^{-1}$ in the intermediate part, and reaching 1 cm y$^{-1}$ values at the top (20–0 cm).

### Sedimentology

The Isoba sedimentary sequence is quite homogenous, mainly composed of organic-rich silts, but changes in sediment colour and texture allows distinguishing several units. The uppermost 65.5 cm of the sequence consist of black massive organic-rich silts (28–0 cm, 35–31.5 cm), light-brownish organic-rich silts with carbonates (31.5–28 cm), banded, dark and light brown, organic-rich silts with carbonates (55–35 cm), banded, dark brown, organic-rich silts with carbonates (65.5–55 cm) (Fig. 2a). The lower part, from 65.5 to 35 cm, feature slightly higher carbonate content and less organic matter than the uppermost section above 35 cm. Organic matter occurs, mainly, as amorphous aggregates with no distinguishable structure. The mineral fraction is composed of abundant subhedral-anhedral calcite crystals (5–15 µm), less abundant euhedral calcite crystals of smaller size (< 5 µm) and frequent quartz grains (5–15 µm), nearly rounded and with wavy extinction. Pyrite framboids are also present at lower abundances.

### Diatom stratigraphy

In total, we identified 39 diatom taxa (corresponding to 17 families and 25 genera), but only 29 taxa reached > 1% in more than one sample (Fig. 3). The most remarkable features of the diatom stratigraphy are the alkaliphilic nature of most taxa, the overall dominance of benthic diatoms in terms of diversity, and the abrupt changes in the composition of the diatom assemblages. Four different DZs were delimited (Fig. 3):

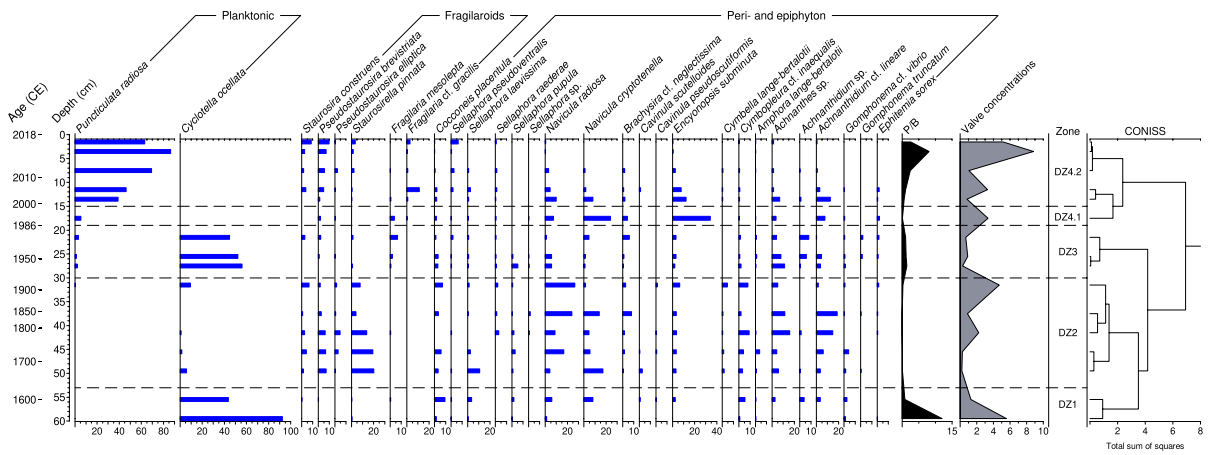


**Fig. 3** Stratigraphic diagram showing changes in the relative abundances (%) of selected diatom taxa (> 1%) from the Isoba record, the P/B Ratio (Planktic-to-Benthic ratio), Valve concentrations (10$^7$ valves g$^{-1}$ dry sediment), Diatom Zones (DZ) and CONISS dendrogram

Diatom Zone 1 (DZ1; 60–53 cm, ~ 1550–1630 CE): absolute diatom concentration is medium–high, varying from 5.6 $10^7$ to 1.3 $10^7$ valves $g^{-1}$. *Cyclotella ocellata* Pantocsek is the dominant taxon with a relative abundance > 90% in the basal zone, decreasing to 43.5% at the top. On the contrary, benthic taxa such as *Cocconeis placentula* Ehrenberg, *Navicula cryptotenella* Lange-Bertalot, *Navicula radiosa* Kützing, *Achnanthes* sp. and *Encyonopsis subminuta* Krammer and Reichardt increase their relative abundances upwards. The planktonic/benthic (P/B) ratio shows a major decrease from 12 to 0.8.

Diatom Zone 2 (DZ2; 53–30 cm, ~ 1630–1925 CE): valve concentration is very low at the bottom (2 $10^6$ valves $g^{-1}$) and increases at the top to 4.7 $10^7$ valves $g^{-1}$. Assemblages change markedly with the dominance, in terms of abundance and diversity, of benthic taxa and the nearly disappearance of *C. ocellata*. Principal species are *N. radiosa* (4.3–26.7%), *Staurosirella pinnata* (Ehrenberg) Williams and Round (4–20.2%), *N. cryptotenella* (1.5–17%) and *Achnanthes* sp. (0–15.8%). Other important species, but with lower abundances, are *Achnanthidium* cf. *lineare* Smith, *Brachysira* cf. *neglectissima* Lange-Bertalot, *Pseudostaurosira brevistriata* (Grunow) Williams and Round, *C. placentula*, *Pseudostaurosira elliptica* (Schumann) Edlund, Morales and Spaulding. P/B ratio drastically descends to values < 0.2, due to the increase in pennate benthic taxa.

Diatom Zone 3 (DZ3; 30–19 cm, 1925–1986 CE): valve concentrations decrease towards the top (to 6.7 $10^6$ valves $g^{-1}$). In compositional terms, planktonic taxa substantially increase at the expense of previously dominant benthic taxa, thus resembling DZ1. *Cyclotella ocellata* increases its relative abundance toward the top to 51% (average), whilst the abundances of the tychoplanktonic *Fragilaria mesolepta* Rabenhorst and the planktonic *Punticulata radiosa* (Grunow) Håkansson increase from bottom to top. Conversely, most benthic taxa such as *N. radiosa*, *E. subminuta*, *Cymbella lange-bertalotii* Krammer and *A.* cf. *lineare* decrease, while *N. cryptotenella* increase. P/B ratio increases upwards to values > 1.

Diatom zone 4 (19–0 cm; 1986–2018 CE): subzone 4.1 (19–15.5 cm; 1986–1997 CE): absolute concentration increases to 3.3 $10^7$ valves $g^{-1}$. Benthic taxa were dominant in terms of abundance and diversity (P/B = 0.05), like in DZ2. This sole assemblage is dominated by *E. subminuta* (34%) and *N. cryptotenella* (24%). Other secondary taxa are *N. radiosa*, *A.* cf. *lineare*, *P. radiosa*, *B.* cf. *neglectissima*, *Achnanthes* sp. and *C. placentula*.

Subzone 4.2 (15.5–0 cm; 1997–2018 CE): this uppermost subzone is markedly different from the lower ones. Valve concentration increases upwards from bottom to 3.5–4.5 cm depth, reaching maximum values (8.82 $10^7$ valves $g^{-1}$). *Puncticulata radiosa* is the dominant taxon, with relative abundances ranging from 39, to 86.4%. Likewise, *Staurosira construens* Ehrenberg reappears and rises up to 8.53%. Benthic taxa have a complex behaviour: certain species like *N. radiosa*, *N. cryptotenella* and *E. subminuta* decrease, whilst *P. brevistriata* and *S. pinnata* display the opposite tendency. At 3.5–4.5-cm depth, *P. radiosa* reaches its maximum abundance coinciding with maximum concentration and high P/B values (8.14). From this depth up, the abundances of *P. radiosa* and the P/B ratio slightly decrease, while abundances of fragilaroid taxa such as *P. brevistriata*, *S. pinnata* and *Fragilaria* cf. *gracilis* Østrup alongside the periphytic and epiphytic taxon *Sellaphora pseudoventralis* (Hustedt) Chudaev & Gololobova increase.

## Statistical analyses

The first two axes of the CA explain more than 62% of the total variance in the Isoba diatom dataset (Fig. 4a). The first axis accounts for 37.5%, while the second one explains 25% of the total variance. The ordination plot allows differentiating three groups associating diatom taxa and samples. Group 1 includes four taxa: *C. ocellata*, *Achnanthidium* sp., *Gomphonema truncatum* Ehrenberg and *F. mesolepta*, and assemblages from the basal and the middle parts of the sequence. Group 2 comprises a large number of species like *N. cryptotenella*, *E. subminuta*, *N. radiosa*, *S. pinnata* and *P. elliptica*, and assemblages from different depths. Finally, Group 3 includes few species (*P. radiosa*, *S. pseudoventralis*, *F.* cf. *gracilis*, *P. brevistriata* and *S. construens*), and the most recent assemblages. The first axis is mainly controlled on its negative side by *P. radiosa*, whereas on its positive side by *C. ocellata*. The second axis is controlled on its positive side by a major group of benthic taxa (including *C. lange-bertalotii* and *Navicula* spp.), and on its negative one by *P. radiosa* and *C. ocellata*. DCA results are mainly explained by the first two axes, which together account more than 85% of

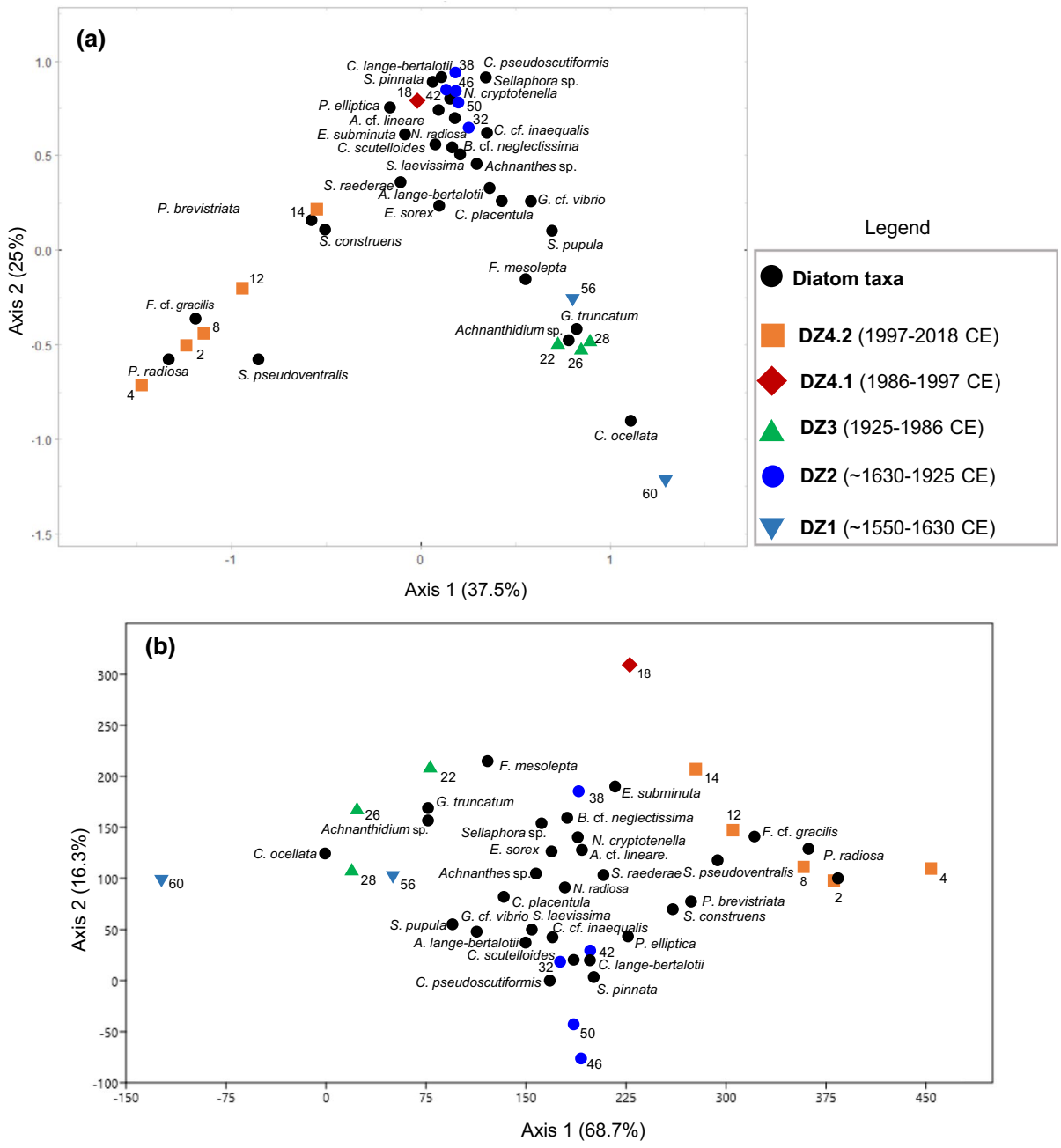


**Fig. 4** **a** Correspondence Analysis (CA; Axis 1 explains 37.5% of the variance, while Axis 2 explains 25% of the variance) and **b** Detrended Correspondence Analysis (DCA; Axis 1 explains 68.7% of the variance, while Axis 2 explains 16.3% of the variance) biplots on the Lake Isoba diatom dataset. The numbers within the biplots represent the mid-point depths of the samples: DZ1 (60, 56), DZ2 (50, 46, 42, 38, 32), DZ3 (28, 26, 22), DZ4.1 (18), DZ4.2 (14, 12, 8, 4, 2)

the total variance. The same three groups can be differentiated and, therefore, DCA results largely agree with those of the CA and thus support the robustness of such analysis (Fig. 4a, b). Similar sample and species distribution in CA and DCA suggests that the arch effect has not distorted our results. Statistical proximities between DZ1 and DZ3 and between DZ2 and DZ4.1 likely indicate

similar environmental conditions governing these diatom assemblages, while the distinctiveness of the uppermost DZ4.2 (15.5–0 cm, 1997–2018 CE) indicates an abrupt turning point of ecological parameters occurring in a very short time.

## Geochemical and compositional proxies

Two main groups of elements can be identified according to their downcore profiles (Fig. 5). On the one hand, Si, Al, K, Zr, Rb, Ti, Sr and Fe show overall decreasing trends from the bottom of the sequence until ~ 50-cm depth and then maintain relatively stable values towards the top. Contrarily, Ca and S display variable values until ~ 39-cm depth, and finally increase their concentrations. The first two axes of the PCA carried out on the elemental geochemistry dataset explain 77.8% of the total variance (Axis 1: 55.4%, Axis 2: 22.4%; Fig. 6). The PCA shows a first group of elements including Ti, Fe, Sr, K, Rb, Al, Zr and Si, which show high positive loads along the axis 1 and are highly positively

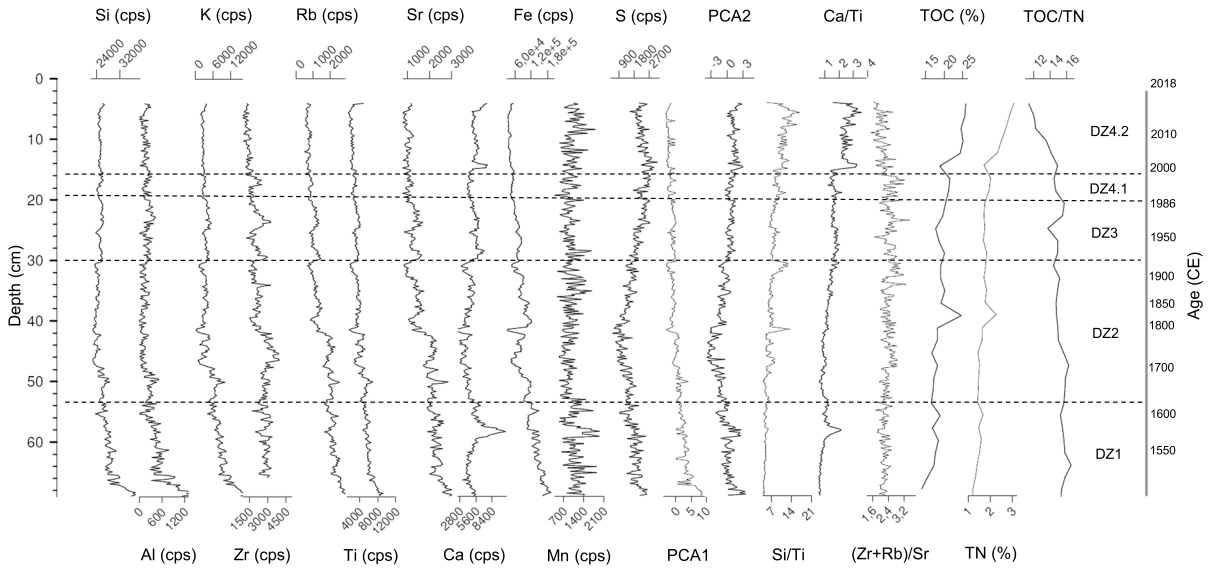


**Fig. 5** Major chemical elements, PCA1 and PCA2 sample scores, selected geochemical ratios and TOC (%), TN (%) and TOC/TN profiles of Isoba

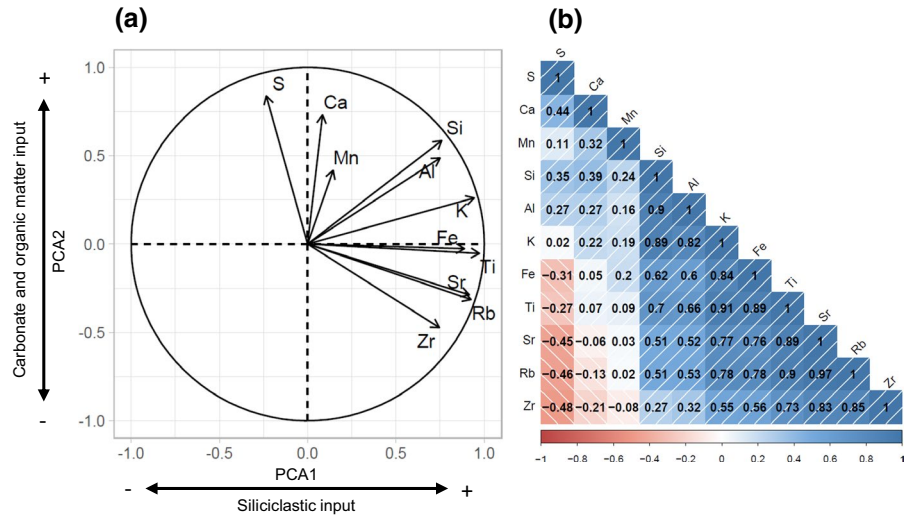


**Fig. 6** **a** Principal Component Analysis (PCA; Axis 1 explains 55.4% of the variance, while Axis 2 explains 22.4% of the variance) and **b** Matrix Correlation of major elements of the Isoba record

correlated among them (Fig. 6), probably because of their presence in the silicate minerals fraction. A second group is represented by Ca, Mn and S, with high loads along the axis 2 and thus barely correlated with the previous elements, and are generally present in carbonatic fraction and organic matter. The first axis (PCA1) shows a slightly decreasing trend from DZ1 (maximum of 7.2) to DZ4.2 (−0.5 to 0; Fig. 5). The second axis (PCA2) decreases from DZ1 to DZ2 (minimum of −3.8 at 47-cm depth), to then increase upwards, reaching a maximum value of 2.8 in DZ4.2 (Fig. 5). Regarding to geochemical ratios, Si/Ti, increases from bottom to top, particularly from the base of DZ4.2 (~1997 CE), coinciding with *P. radiosa* peak abundance and maximum absolute concentrations of diatom valves. Ca/Ti ratio displays a similar spectrum to Si/Ti, except for a small positive peak at ~58 cm depth in DZ1, increasing particularly in the uppermost 15 cm, coinciding with DZ4.2 (~1997 CE). (Zr + Rb)/Sr ratio presents a decreasing trend towards the top, particularly at the beginning of DZ4.2.

The organic matter content is variable but relatively high throughout the record (Fig. 5). TOC shows increasing values from DZ1 to DZ4.1 (from ~15 to > 20%), with a remarkable further increase (to ~25%) at the beginning of DZ4.2 (~1997 CE). The TN curve largely runs parallel to the TOC. There is a marked decrease in the atomic ratio TOC/TN (from ~15 to ~11) in the DZ4.2 (~1997–2018 CE).

## Discussion

The diatom, geochemical and sedimentological data from the Isoba sequence provide a robust multiproxy palaeoenvironmental reconstruction for the past ~500 years on the southern slopes of the Cantabrian Mountains (Fig. 7).

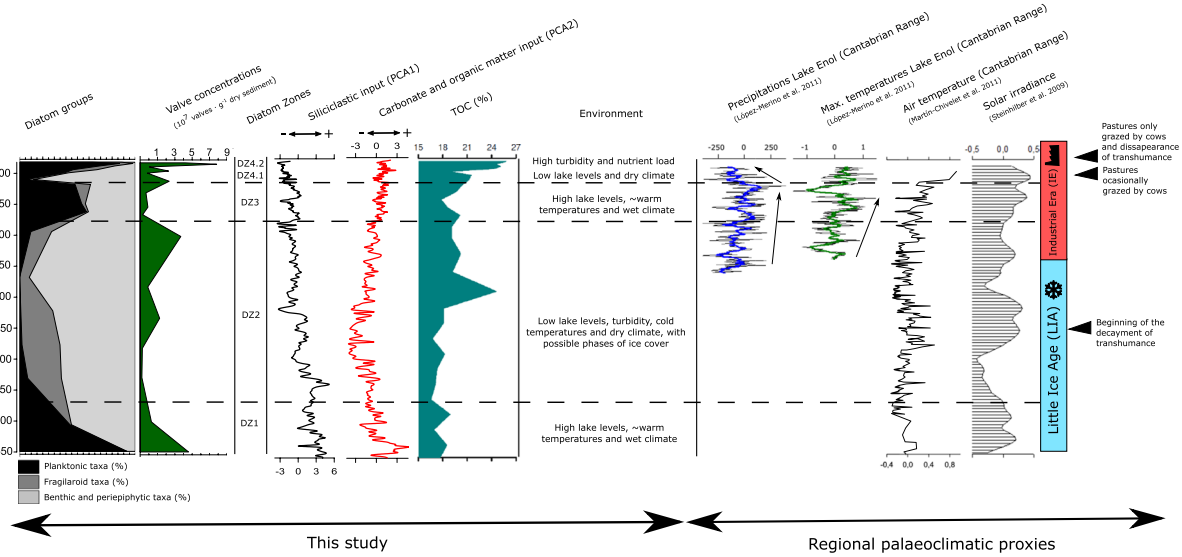


**Fig. 7** Abundances of the main groups of diatoms (Planktonic, Fragilaroid, Benthic, periphytic and epiphytic taxa; %), Valve concentrations, Diatom Zones (DZ), PCA axis 1 (PCA1) and axis 2 (PCA2) sample scores of the geochemical record, TOC (%), Environmental conditions inferred for Lake Isoba, Precipitation and Maximum Temperature in Lake Enol (López-Merino et al. 2011), Air temperature (Martín-Chivelet et al. 2011), Solar Irradiance (Steinhilber et al. 2009) and historical information of transhumance

### The Little Ice Age and the onset of the Industrial Era (~ *1550 to 1925 CE)*

The high abundance of the planktonic *C. ocellata* during DZ1 and the variable presence of benthic periphytic and epiphytic taxa (such as *C. placentula*, *N. radiosa* and *N. cryptotenella*) suggest predominant warm-wet summers conditions and variable macrophyte coverage at ~ 1550 to 1630 CE (Smol et al. 1991; Catalán et al. 2002). Likewise, lake levels were probably high in general, yet featured oscillations. Also, stable conditions in terms of windiness cannot be excluded (Reavie et al. 2016). The results of ordination analyses also support the occurrence of notable lake-level fluctuations, considering the distance between the major group of benthic diatoms and the planktonic taxa. Seasonal blooms of *C. ocellata*, favoured by warm water temperatures (> 10 °C to thrive) (Stoermer and Ladewski 1976) and possibly high phosphorous concentrations in the water column (Rojo et al. 1999), might explain the medium to high diatom valve productivity (concentration) scores recorded. The results of the ordination analyses indicate that water transparency-turbidity and nutrient load may have experienced significant variability during the past few centuries, given that the only two planktonic taxa at Isoba, *C. ocellata* and *P. radiosa*, are located on opposed extremes along the axis 1. *Cyclotella ocellata* is usually found in clear waters, whereas *P. radiosa* is associated with more turbid environments and productive waters (Rimet et al. 2009; Naeher et al. 2012). In this period, the great abundance of *C. ocellata* together with the secondary presence of *G. truncatum*, *A.* cf. *lineare*. *N. radiosa*, *Sellaphora laevissima* (Kützing) Mann and *Cymbopleura* cf. *inaequalis* (Ehrenberg) Krammer point to variable nutrient loads, which is consistent with the absolute valve concentrations and variable organic matter content. Besides, PCA1, PCA2 and the (Zr + Rb)/Sr ratio (all indicative of siliciclastic vs. carbonatic input) point to relatively high siliciclastic and carbonate inputs between ~ 1550 to 1630 CE probably associated with higher surface runoff under relatively moister climatic conditions.

The significant changes observed in the diatom assemblages during the period ~ 1630 to 1925 CE can be related to hydrological changes. In DZ2, periphytic and epiphytic taxa (like *Navicula radiosa*, *S. laevissima*, *S. pupula* or *N. cryptotenella*) are dominant over planktonic species indicating greater macrophyte development than during DZ1. Further, the low abundances of planktonic and the abundance of benthic taxa indicate relatively low lake levels between ~ 1630 and 1925 CE. The maximum abundances of small fragilaroids (*S. pinnata*, *P. brevistriata*) that are common in Arctic systems (Rühland and Smol 2002) suggest the occurrence of prolonged periods of ice cover. The proliferation of these taxa has been recorded in shallow lakes at high elevation under cold conditions (Karst-Riddoch et al. 2009), generally with oligotrophic and turbid waters (Rühland and Smol 2002; Rühland et al. 2015). Although, the occurrence of *S. pinnata* has been linked to shallow and turbid environments with important minerogenic inputs (Hall et al. 2003), the relatively low PCA1 values in the geochemistry dataset indicate that siliciclastic input was only moderate during this period. Therefore, from the diatom assemblages we can infer shallower lake levels under colder conditions. The shallow lake would have been more exposed to wind, which would in turn have increased water turbidity.

The slight increase of periphytic and epilithic taxa suggest an expansion of lacustrine nearshore environments, which occurs in lakes with certain basin morphology when lower water level decreases (Morellón et al. 2011). Diatom-inferred predominantly lower water levels between ~ 1630 and 1925 CE correlate with lower siliciclastic input. Taken together, our data indicate relatively dry climatic conditions with reduced surface runoff and therefore limited siliciclastic input.

In the Iberian Peninsula, the Little Ice Age (LIA; 1300–1850 CE) was characterised by general temperature decreases and substantial hydrological variability, whose environmental effects are broadly recorded in mountain lakes (Morellón et al. 2011, 2012; López-Merino et al. 2011; Roberts et al. 2012). Considering the ages estimated for the bottom section of the studied record, DZ1 (~ 1550 to 1630 CE) and DZ2 (~ 1630 to 1925 CE) match the middle and late periods of the LIA and the onset of the Industrial Era. Palaeoclimatic records from glacial, lake and peat deposits and speleothems reveal an overall cold and wet climatic context in the Cantabrian Mountains during late sixteenth and early seventeenth centuries CE, with particularly cold spells intercalated (Oliva et al. 2018), coinciding with records from Sierra Nevada, the Pyrenees and

the Iberian Central Range (Morellón et al. 2012; Oliva et al. 2018) as well as elsewhere in the Mediterranean realm and Europe (Calò et al. 2013). Late sixteenth and early seventeenth centuries CE in NW Iberian Peninsula (Chao de Veiga Mol raised bog) were described as mainly wet and cold but with several dry episodes (Castro et al. 2020). However, according to the multi-proxy evidence presented here, the ~ 1550 to 1630 CE period is characterised by relatively wet, and not particularly cold conditions. This period therefore possibly coincides with one of the warmer events that punctuated the generally cold LIA in northern Spain (Martín-Chivelet et al 2011). The inferred high lake levels were probably promoted by higher rainfall. In the Pyrenees, most studied lakes also indicated a prevalence of relatively humid conditions at that time (Morellón et al. 2012).

The Isoba record indicated that lower water levels, siliciclastic input and primary productivity, as well as high turbidity prevailed between ~ 1630–1925 CE. These changes probably occurred in response to a shift towards colder and drier conditions, likely connected to variability in solar irradiance (Crowley 2000; Steinhilber et al. 2009). High water turbidity reconstructed at Isoba is also synchronous with extreme and prolonged droughts and storms recorded in Iberia (Barriendos 1997). The intensification of extreme events could be related with strong alterations in wind patterns, favouring turbidity in the context of shallow lake levels. Cold temperatures during the last decades of the LIA have also been recorded in Lake Enol (Fig. 1; López-Merino et al. 2011). Nevertheless, the high abundances of plankton recorded in Lake Enol (López-Merino et al. 2011) contrast with the near absence of plankton and the dominance of periphytic and epiphytic taxa and small fragilaroids in Isoba at ~ 1630–1925 CE. The location of Isoba on the drier southern slopes of the Cantabrian Mountains might be responsible for the shallower conditions. Palaeoenvironmental reconstructions and documentary records from NW Iberia also indicate a clear tendency towards colder and drier conditions during the late seventeenth and early eighteenth centuries CE (Fernández Cortizo 2016; Castro et al. 2020). Furthermore, temperature inferences from Isoba agree with previous reconstructions from the Cantabrian Mountains (speleothems; Martín-Chivelet et al. 2011) and the Pyrenees (tree rings; Dorado Liñán et al. 2012).

### The Industrial Era (1925 CE–present day)

The reappearance and abrupt rise of *C. ocellata* in DZ3 (1925–1986 CE), still sharing the lake with a diverse periphytic and epiphytic assemblage indicates a major shift in the hydrological conditions of Isoba towards relatively higher water levels and warmer conditions. Higher abundances of this taxon were also recorded in Lake Enol during the period 1880–1960 CE, coinciding with an increase in precipitation of 16.9 mm/decade (López-Merino et al. 2011). At Isoba, this period is also characterised by higher carbonate content (Fig. 5), whose origin could have been either from detrital input associated to erosion in the catchment (mostly on calcareous bedrock; Fig. 1c) or precipitation of endogenic carbonates, favoured by warmer conditions, as often recorded in lake basins (Wetzel 2001).

A warming trend starting at the end of the LIA at ~ 1850 CE has been reconstructed in other areas of the Cantabrian Mountains from speleothem and lake records (López-Merino et al. 2011; Martín-Chivelet et al. 2011) and elsewhere in the Mediterranean (Calò et al. 2013). Cantabrian glaciers also shrank quickly until their complete disappearance during the first half of the twentieth century CE, coinciding with a considerable reduction of other Iberian glaciers (Oliva et al. 2018; Serrano et al. 2018). Nutrient and organic matter content inferred from diatom assemblages' composition and productivity in Isoba together with a slight increase in TOC and TN, probably reflect an increase in the nutrient load. Since the thirteenth century CE, the lake catchment and its surroundings were used for grazing by long-distance transhumant flocks of merino sheep (Ezquerra and Rey 2011), a widespread activity in the Cantabrian Mountains, particularly on south-facing areas like Isoba (Rodríguez 2001; Carracedo 2018). In fact, Isoba is located inside an ancient pasture plot named "Peña" (245 ha), traditionally rented by transhumant shepherds for summer grazing until 2010 CE, when transhumant flocks were substituted by local cattle (Rodríguez 2001; Ezquerra and Rey 2011). Consequently, the peak in primary productivity at the base of DZ3, indicated by absolute valve concentrations and the slight increase in TOC, might have been related to the impact of livestock around Isoba, favoured by shorter seasonal snow cover due to warmer conditions in the region associated with the end of the LIA.

Diatom assemblages changed abruptly in DZ4.1 (1986–1997 CE) towards a clear dominance of benthic, periphytic and epiphytic taxa, suggesting an extensive macrophyte cover. Valve concentration values suggest moderate primary productivity. This shift can be attributed to relatively lower lake levels resulting from a regional decrease in precipitation over the Cantabrian Mountains. According to the instrumental record from the northern slope of these mountains, a negative anomaly in precipitation has occurred since 1976 CE synchronous with a rise of 0.29 °C/decade in maximum temperatures (López-Merino et al. 2011). A similar increase was also recorded in a speleothem record from the southern Cantabrian Mountains (Martín-Chivelet et al. 2011). Therefore, increased productivity from low (in DZ3) to medium levels (in DZ4.1) can be a response to warmer temperatures (López-Merino et al. 2011).

Finally, a noticeable change in diatom assemblages occurred in DZ4.2 (1997–2018 CE), indicative of a major shift in the ecological status during the past two decades. The persistence of numerous periphytic and epiphytic taxa (like *E. subminuta*, *N. cryptotenella* and *A.* cf. *lineare*) indicate a well-developed macrophytic vegetation, but with different hydrological characteristics, as suggested by Fernández-Aláez et al. (1987). Most of the taxa are alkaliphilic (Van Dam et al. 1994), pointing to high lake carbonate water content. High abundances of small fragilaroids (*S. construens* and *P. brevistriata*) alongside the clear dominance of *P. radiosa* reflect relatively high turbidity in the water column along DZ4.2 (Kuefner et al. 2020), coinciding with rising sedimentation rates, carbonate input and abrupt increase in organic matter since ~ 1997 CE (Fig. 5). *Puncticulata radiosa* mostly spreads during late summer and autumn under high nutrient concentration and turbulent regimes (Morabito et al. 2002; López-Merino et al. 2011) and has been found in productive waters and low light conditions in European mountain lakes (Rimet et al. 2009; López-Merino et al. 2011; Naeher et al. 2012). Increasing runoff and warmer conditions might have favoured a general rise in sediment input and organic matter. Despite the main process is the accumulation of organic matter (Fig. 5), more intense weathering and erosion of limestones from the lake catchment might contribute to explain the raise in the carbonate fraction (Wetzel 2001).

Higher nutrient input in Isoba during the period 1997–2018 CE likely led to increasing diatom productivity, as indicated by absolute valve concentrations, Si/Ti (indicative of biogenic and detrital Si vs siliciclastic sediment fraction) and TOC/TN. The increase in Si/Ti in DZ4.2 does not match the lower siliciclastic input represented by PCA1, likely indicating a predominantly biogenic source of Si related with higher primary productivity (Peinerud 2000). This would agree with the probable algal origin of the organic matter according to its microscopic characteristics (Kelts 2003) and the marked decrease in the atomic ratio TOC/TN (Meyers and Lallier-Vergès 1999). Nutrient enrichment has become a major stressor in mountain lakes, able to deteriorate their ecological status and disrupt natural dynamics. A limnological survey carried out in Isoba in the late 1980s CE (Fernández-Aláez et al. 1987) evidenced a loss of oligotrophy, as inferred from macrophyte analysis but particularly from the presence of a large helophytic belt around the lake and the expansion of submerged vegetation. According to our chronology, this process did not have a noticeably impact in the diatom communities of Isoba until 1997 CE and peaked after 2010 CE.

Transhumant sheep grazing in the Cantabrian Mountains declined significantly during the 1990s–2000s CE (Ezquerra et al. 2005; Ezquerra and Rey 2011). This traditional use remains in a few plots but around Isoba was definitely substituted by local cattle since ~ 2010 CE. The replacement of summer-grazing sheep flocks with staying cattle implied severe changes on water bodies. Transhumant merino sheep were constantly moving driven by shepherds throughout the lake catchment and its surroundings, while staying cattle is subject to almost no management and, besides, its presence longer. Excessive water lapping in cattle can lead to formation of muddy bogs around water troughs (Moran and Doyle 2015) and their more frequent access to water can significantly increase turbidity in lakes by suspending fine sediments (Burt et al. 2013). Furthermore, their preferential behaviour to defecate in streams and lakes increases their organic and nutrient loads (Bond et al. 2014). The impact of faecal pollution from cattle on diatom communities in lakes has also been reported, both in compositional and diversity terms (Burt et al. 2013). In fact, the disruption of the trophic status has been found to be more significant in small lakes

with a reduced drainage area (Catalán et al. 1993), as occurs at Isoba. Therefore, the increase in grazing by local cattle since 1997 CE—replacing completely the sheep transhumant flocks since 2010 CE—around Isoba, is likely to have caused the nutrient enrichment and turbidity increase leading to the abrupt change in diatom assemblages in recent times.

## Conclusions

The multidisciplinary study of the sedimentary sequence from Lake Isoba, based on diatoms, high-resolution elemental geochemistry, compositional proxies and sedimentology has allowed a precise reconstruction of the environmental and hydrological history of the Cantabrian Mountains during the past ~ 500 years.

Diatom stratigraphy depicted abrupt changes largely controlled by the shallow character and local geological features of the lake. Four main periods characterised by different environmental conditions and driven by the interplay between climate fluctuations and human activities have been reconstructed.

The middle period of the LIA (~ 1550 to 1630 CE) is characterised by high lake levels, enhanced runoff and medium to high primary productivity, determined by wet conditions. Conversely, the last period of the LIA and the onset of the Industrial Era (~ 1630 to 1925 CE) is characterised by lower lake levels, decreasing clastic input, higher water turbidity and low primary productivity, likely induced by an overall cold and dry climate, as reconstructed in other records from the Cantabrian Mountains. However, comparatively drier conditions with respect to other records of the Northern Cantabrian Mountains occurred in Isoba during this period likely because of its location in the southern slope. The Industrial Era in the twentieth century is reflected by higher lake levels and increasing sediment input, nutrients and organic matter caused by warmer temperatures and more humid conditions.

A regional decrease in precipitation after 1986 CE likely caused a shift towards the dominance of periphytic and epiphytic diatom taxa in the context of lower lake levels. Finally, the period 1997–2018 CE was characterised by a strong anthropic impact driven by the introduction of local cattle at the expense of the traditional transhumant sheep flocks and determined a major hydrological and environmental shift marked by higher sediment input and water turbidity, and a drastic increase in primary productivity, organic matter and nutrients detected since 1997 CE, in the context of substantial land use changes.

In summary, the recent sedimentary record from Lake Isoba demonstrates the high sensitivity of diatom species and communities of mountain lakes to subtle climate changes. Additionally, this study has shown that diatom communities and species rapidly react to hydrological variations caused by local and global anthropogenic disturbances. The comprehensive analysis and the understanding of the interplay between climate and human activities during past decades would help to manage and restore current anthropized and threatened mountain lakes.

**Acknowledgements** This research was funded by the GECANT project "Climate and human drivers in the geoenvironmental evolution of the Cantabrian Region during the Anthropocene: integrating coastal, mountain lake and geomorphological records (CGL2017-82703-R) (AEI/FEDER, UE)", the University of Bern and a 'María Zambrano' fellowship (Ministerio de Universidades/Universidad de Alcalá/European Union) to C.M-M. We thank the 'Junta de Castilla y León' ('Servicio Territorial de Medio Ambiente de León') and the administration of "Montañas de Riaño y Mampodre" Regional Park for issuing the permits to core Lake Isoba. André F. Lotter, Erika Gobet, Christoph Schwörer (University of Bern), Carlos Sierra-Fernández (University of León), Diego Baragaño (INDUROT-University of Oviedo), Santiago de Castro, María Galán, Mariano Torre (Junta de Castilla y León), Toño Barreda, Jaime Bonachea, Luis Echeandía, Lucía Agudo, Ana Belén Marín, Ignacio Varela (University of Cantabria), Elena Royo, Raquel López, Miguel Bartolomé, Alejandra Vicente de Vera, Blas Valero-Garcés (IPE-CSIC), Jaime Frigola (University of Barcelona), Lucía Arregui (Complutense University of Madrid), Aida Adsuar (IGEO-CSIC-UCM), Javier Sigró (Rovira i Virgili University) and Javier Martín-Chivelet (Complutense University of Madrid) are kindly acknowledged for their help with fieldwork, search for historical information and laboratory analyses. Thanks to the editors and two anonymous reviewers for their valuable comments and suggestions that contributed to improve the article.

**Funding** Open Access funding provided thanks to the CRUE-CSIC agreement with Springer Nature. Open Access funding provided by University of the Basque Country. This study was financially supported by the GECANT project (CGL2017-82703-R) (AEI/FEDER, UE).

## References

Álvarez-Marrón J, Pérez-Estaún A, Aller N, Heredia N (1988) Mapa geológico y Memoria de la Hoja nº 79/14-06 (Puebla de Lillo). Mapa Geológico De España e 1(50):000

Appleby PG (2001) Chronostratigraphic techniques in recent sediments. In: Smol JP, Birks HJB, Last WM (eds) Tracking environmental change using lake sediments, volume 1: basin analysis, coring and chronological technique. Kluwer Academic Publishers, Dordrecht, pp 171–203

Barriendos M (1997) Climatic variations in the Iberian Peninsula during the late Maunder Minimum (AD 1675–1715): an analysis of data from rogation ceremonies. Holocene 7(1):105–111

Battarbee RW (1986) Diatom analysis. In: Berglund BE (ed) Handbook of holocene palaeoecology and palaeohydrology. Wiley, Chichester, pp 527–570

Battarbee RW, Jones VJ, Flower RJ, Cameron NG, Bennion H, Carvalho L, Juggins S (2001) Diatoms. In: Smol JP, Birks HJB, Last WM (eds) Tracking environmental change using lake sediments, volume 3: terrestrial, algal and siliceous indicators. Kluwer Academic Publishers, Dordrecht, pp 155–202

Blaauw M, Christen JA, Vazquez JE, Goring S (2020) Classical age-depth modelling of cores from deposits v. 2.3.7, https://CRAN.R-project.org/package=clam; searched on 27 November 2020

Bond T, Sear D, Sykes T (2014) Estimating the contribution of in-stream cattle faeces deposits to nutrient loading in an English chalk stream. Agric Water Manag 131:156–162

Burt C, Bachoon DS, Manoylov K, Smith M (2013) The impact of cattle farming best management practices on surface water nutrient concentrations, faecal bacteria and algal dominance in the Lake Oconee watershed. Water Environ J 27:207–215

Calò C, Henne PD, Eugster P, van Leeuwen J, Gilli A, Hamann Y, La Mantia T, Pasta S, Vescovi E, Tinner W (2013) 1200 years of decadal-scale variability of Mediterranean vegetation and climate at Pantelleria Island, Italy. Holocene 23:1477–1486

Carracedo V, Cunill R, García-Codrón JC, Pèlachs A, Pérez-Obiol R, Soriano JM (2018) History of fires and vegetation since the Neolithic in the Cantabrian Mountains (Spain). Land Degrad Dev 29:2060–2072

Castro D, Souto M, Fraga MI, García-Rodeja E, Pérez-Díaz S, López Sáez JA, Pontevedra-Pombal X (2020) High-resolution patterns of palaeoenvironmental changes during the Little Ice Age and the Medieval Climate Anomaly in the northwestern Iberian Peninsula. Geosci Front 11(5):1461–1475

Catalán J, Ballesteros E, Gacia E, Palau A, Camarero L (1993) Chemical composition of disturbed and undisturbed high-mountain lakes in the Pyrenees: a reference for acidified sites. Water Res 27(1):133–141

Catalán J, Pla S, Rieradevall M, Felip M, Ventura M, Buchaca T, Camarero L, Brancelj A, Appleby PG, Lami A, Grytnes JA, Agustí-Panareda A, Thompson R (2002) Lake Redó ecosystem response to an increasing warming in the Pyrenees during the twentieth century. J Paleolimnol 28:129–145

Cohen AS (2003) Paleolimnology: the history and evolution of lake systems. Oxford University Press, United States

Crowley TJ (2000) Causes of climate change over the past 1000 years. Science 289:270–277

Dorado Liñán I, Büntgen U, González-Rouco F, Zorita E, Montávez JP, Gómez-Navarro JJ, Brunet M, Heinrich I, Helle G, Gutiérrez E (2012) Estimating 750 years of temperature variations and uncertainties in the Pyrenees by tree-ring reconstructions and climate simulations. Clim past 8:919–933

Ezquerra FJ, Rey R (2011) La evolución del paisaje vegetal y el uso del fuego en la Cordillera Cantábrica. Fundación Patrimonio Natural de Castilla y León, Valladolid

Ezquerra FJ, García JC, Ramírez J (2005) Principales conclusiones del estudio de caracterización de los puertos pirenaicos de la provincia de León. In: Libro de Resúmenes, Conferencias y Ponencias. 4º Congreso Forestal Español: 4CFE05–370-T1, SECF-Gobierno de Aragón (Eds.): 332. Imprenta Repes, S.C. Zaragoza

Fernández Cortizo C (2016) La Pequeña Edad de Hielo en Galicia: Estado de la cuestión y estudio histórico. Obradoiro De Historia Moderna 25:9–39

Fernández-Aláez M, Luis Calabuig E, Fernández-Aláez C (1987) Análisis y distribución de la vegetación macrófita en lagos de montaña de la provincia de León. Lazaroa 7:221–233

Guiry MD, Guiry GM (2020) AlgaeBase. World-wide electronic publication, National University of Ireland, Galway. https://www.algaebase.org; searched on 20 August 2020

Hall RI, Wolfe BB, Edwards TWD, Karst-Riddoch TL, Vardy S, McGowan S, Sjunneskog C, Paterson A, Last W, English M, Sylvestre F, Leavitt PR, Warner BG, Boots B (2003) A multi-century flood, climatic and ecological history of the peace-athabasca delta. Northern Alberta, Canada. BC Hydro Technical Report

Jambrina-Enríquez M, Rico M, Moreno A, Leira M, Bernárdez P, Prego R, Recio C, Valero-Garcés B (2014) Timing of deglaciation and postglacial environmental dynamics in NW Iberia: the Sanabria Lake record. Quat Sci Rev 94:136–158

Karst-Riddoch TL, Malmquist HJ, Smol JP (2009) Relationships between freshwater sedimentary diatoms and environmental variables in Subarctic Icelandic lakes. Arch Hydrobiol 175(1):1–28

Kelts KR (2003) Components in lake sediments. Smear slide identifications. In: Valero-Garcés BL (ed) Limnogeología en España: un tributo a Kerry Kelts. Biblioteca de Ciencias (CSIC), pp 59–72

Krammer K, Lange-Bertalot H (1986–1991) Bacillariophyceae. In: Ettl H, Gerloff J, Heynig H, Mollenhauer D (eds) Süßwasserflora von Mitteleuropa 1-4. Gustav Fischer Verlag, Stuttgart & New York

Kuefner W, Hofmann A, Ossyssek S, Dubois N, Geis J, Raeder U (2020) Composition of a highly diverse diatom community shifts as response to climate change: a down core study of 23 central European mountain lakes. Ecol Indic 117:106590

Lange-Bertalot H (2000–2005) Diatoms of the European inland waters and comparable habitats. Volumes 1, 2, 3, 4, 5. ARG. Gantner Verlag, Ruggell, Liechstenstein

López-Merino L, Moreno A, Leira M, Sigró J, González-Sampériz P, Valero-Garcés B, López-Sáez JA, Brunet M, Aguilar E (2011) Two hundred years of environmental change in Picos de Europa National Park inferred from sediments of Lago Enol, northern Iberia. J Paleolimnol 46:453–467

Martín-Chivelet J, Muñoz-García MB, Edwards RL, Turrero MJ, Ortega AI (2011) Land surface temperature changes in Northern Iberia since 4000 yr BP, based on $\delta^{13}C$ of speleothems. Glob Planet Change 77:1–12

Meyers PA, Lallier-Vergès E (1999) Lacustrine sedimentary organic matter records of late quaternary paleoclimates. J Paleolimnol 21:345–372

Morabito G, Ruggiu D, Panzani P (2002) Recent dynamics (1995–1999) of the phytoplankton assemblages in Lago Maggiore as a basic tool for defining association patterns in the Italian deep lakes. J Paleolimnol 61:129–145

Moran J, Doyle R (2015) Cow talk: understanding dairy cow behaviour to improve their welfare on Asian farms. CSIRO Publishing. https://doi.org/10.1071/9781486301621

Morellón M, Valero-Garcés B, González-Sampériz P, Vegas-Vilarrúbia T, Rubio E, Rieradevall M, Delgado-Huertas A, Mata P, Romero O, Engstrom DR, López-Vicente M, Navas A, Soto J (2011) Climate changes and human activities recorded in the sediments of Lake Estanya (NE Spain) during the Medieval Warm Period and Little Ice Age. J Paleolimno 46:423–452

Morellón M, Pérez-Sanz A, Corella JP, Büntgen U, Catalán J, González-Sampériz P, González-Trueba JJ, López-Sáez JA, Moreno A, Pla-Rabes S, Saz-Sánchez MÁ, Scussolini P, Serrano E, Steinhilber F, Stefanova V, Vegas-Vilarrúbia T, Valero-Garcés B (2012) A multi-proxy perspective on millennium-long climate variability in the Southern Pyrenees. Clim past 8:683–700

Moreno A, López-Merino L, Leira M, Marco-Barba J, González-Sampériz P, Valero-Garcés B, López-Sáez JA, Santos L, Mata P, Ito E (2011) Revealing the last 13,500 years of environmental history from the multiproxy record of a mountain lake (Lago Enol, northern Iberian Peninsula). J Paleolimnol 46:327–349

Naeher S, Smittenberg RH, Gilli A, Kirilova EP, Lotter AF, Schubert CJ (2012) Impact of recent lake eutrophication on microbial community changes as revealed by high resolution lipid biomarkers in Rotsee (Switzerland). Org Geochem 49:86–95

Niyatbekov T, Barinova SS (2018) Bioindication of aquatic habitats with diatom algae in the Pamir Mountains, Tajikistan. MOJ Ecol Environ Sci 3(3):117–120

Oliva M, Ruiz-Fernández J, Barriendos M, Benito G, Cuadrat JM, Domínguez-Castro F, García-Ruiz JM, Giralt S, Gómez-Ortiz A, Hernández A, López-Costas O, López-Moreno JI, López-Sáez JA, Martínez-Cortizas A, Moreno A, Prohom M, Saz MA, Serrano E, Tejedor E, Trigo R, Valero-Garcés B, Vicente-Serrano SM (2018) The Little ice age in Iberian mountains. Earth-Sci Rev 177:175–208

Ortega Villazán MT, Morales Rodríguez CG (2015) El clima de la Cordillera Cantábrica castellano-leonesa: diversidad, contrastes y cambios. Investigaciones Geográficas 63:45–67

Peinerud EK (2000) Interpretation of Si concentrations in lake sediments: three case studies. Environ Geol 40(1–2):64–72

Reavie ER, Sgro GV, Estepp JR, Bramburger AJ, Shaw Chraibi VL, Pillsbury RW, Cai M, Stow CA, Dove A (2016) Climate warming and changes in Cyclotella sensu lato in the Laurentian Great Lakes. Limnol Oceanogr 62(2):768–783

Reimer PJ, Austin WEN, Bard E, Bayliss A, Blackwell PG, Ramsey CB, Butzin M, Cheng H, Edwards RL, Friedrich M, Grootes PM, Guilderson TP, Hajdas I, Heaton TJ, Hogg AG, Hughen KA, Kromer B, Manning SW, Muscheler R, Palmer JG, Pearson C, van der Plicht J, Reimer RW, Richards DA, Scott EM, Southon JR, Turney CSM, Wacker L, Adolphi F, Büntgen U, Capano M, Fahrni SM, Fogtmann-Schulz A, Friedrich R, Köhler P, Kudsk S, Miyake F, Olsen J, Reinig F, Sakamoto M, Sookdeo A, Talamo S (2020) The IntCal20 Northern hemisphere radiocarbon age calibration curve (0–55 cal kBP). Radiocarbon 62(4):725–757

Renberg I (1990) A procedure for preparing large sets of diatom slides from sediment cores. J Paleolimnol 4:87–90

Reynolds CS (2006) Ecology of phytoplankton. Cambridge University Press, Cambridge

Rimet F, Druart JC, Anneville O (2009) Exploring the dynamics of plankton diatom communities in Lake Geneva using emergent self-organizing maps (1974–2007). Ecol Inform 4:99–110

Roberts N, Moreno A, Valero-Garcés BL, Corella JP, Jones M, Allcock S, Woodbridge J, Morellón M, Luterbacher J, Xoplaki E, Türkeş M (2012) Palaeolimnological evidence for an east-west climate see-saw in the Mediterranean since AD 900. Glob Planet Change 84–85:23–34

Rodríguez M (2001) La Trashumancia. Cultura, cañadas y viajes. Edilesia, León, España

Rojo C, Kiss KT, Álvarez-Cobelas M, Rodrigo MA (1999) Population dynamics of Cyclotella ocellata (Bacillariophyceae): endogenous and exogenous factors. Arch Hydrobiol 145(4):479–495

Rühland KM, Smol JP (2002) Freshwater diatoms from the Canadian arctic treeline and development of paleolimnological inference models. J Phycol 38(2):249–264

Rühland KM, Paterson AM, Smol JP (2015) Diatom assemblage responses to warming: reviewing the evidence. J Paleolimnol 54:1–35

Schnurrenberger D, Russell J, Kelts K (2003) Classification of lacustrine sediments based on sedimentary components. J Paleolimnol 29:141–154

Serrano E, Oliva M, González-García M, López-Moreno JI, González-Trueba J, Martín-Moreno R, Gómez-Lende M, Martín-Díaz J, Nofr J, Palma P (2018) Post-little ice age paraglacial processes and landforms in the

high Iberian mountains: a review. Land Degrad Dev 29(11):4186–4208
Smol JP, Walker IR, Leavitt PR (1991) Paleolimnology and hindcasting climatic trends. Int Ver Theor Angew Limnol Verh 24(2):1240–1246
Steinhilber F, Beer J, Fröhlich C (2009) Total solar irradiance during the Holocene. Geophys Res Lett 36:L19704
Stoermer EF, Ladewski TB (1976) Apparent optimal temperatures for the occurrence of some common phytoplankton species in southern Lake Michigan. J Great Lakes Res 18:49
Stoermer EF, Smol JP (1999) The Diatoms: applications for the environmental and earth sciences. Cambridge University Press, Cambridge
Van Dam H, Mertens A, Sinkeldam J (1994) A coded checklist and ecological indicator values of freshwater diatoms from the Netherlands. Neth J Aquat Ecol 28:117–133
Vegas-Villarrúbia T, González-Sampériz P, Morellón M, Gil-Romera G, Pérez-Sanz A, Valero-Garcés B (2013) Diatom and vegetation responses to Late Glacial and Early Holocene climate changes at Lake Estanya (Southern Pyrenees, NE Spain). Palaeogeogr Palaeoclimatol Palaeoecol 392:335–349
Wetzel RG (2001) Limnology. Lake and river ecosystems, 3rd edn. Academic Press